

07.3;13.1

Photosensitivity of a metal–insulator–semiconductor field-effect transistor based on PbSnTe:In film with a composition close to the bands inversion

© A.E. Klimov^{1,2}, I.O. Akhundov¹, V.A. Golyashov^{1,3}, D.V. Gorshkov¹, D.V. Ishchenko¹, G.Yu. Sidorov¹, N.S. Pashchin¹, S.P. Suprun¹, A.S. Tarasov¹, E.V. Fedosenko¹, O.E. Tereshchenko^{1,3}

¹Rzhanov Institute of Semiconductor Physics, Siberian Branch, Russian Academy of Sciences, Novosibirsk, Russia

²Novosibirsk State Technical University, Novosibirsk, Russia

³Novosibirsk State University, Novosibirsk, Russia

E-mail: klimov@isp.nsc.ru

Received November 14, 2022

Revised November 14, 2022

Accepted November 30, 2022

A prototype of a metal–insulator–semiconductor field-effect transistor based on PbSnTe:In/(111)BaF₂ film with an Al₂O₃ gate dielectric was designed for the first time. With the gate voltage applied in the range $-7.7 < U_{gate} < +7.7$ V the relative modulation in the drain-source current $\Delta I_{ds}/I_{ds}$ attained near five-fold change at $T = 4.2$ K. When illuminated with relatively low (~ 100 photon/s) fluxes, negative photoconductivity was detected accompanied with a decrease in I_{ds} by $\sim 10^4$ times and a simultaneous decrease in ΔI_{ds} by $\sim 10^3$ times or even more. The estimated detectivity was about $\sim 7 \cdot 10^{16}$ cm · Hz^{0.5} · W⁻¹ at a wavelength λ about 25 micron with the accumulation time about 0.5 s. A qualitative model is discussed which assumes the existence of deep traps and a photo-capacitance effect.

Keywords: Epitaxial films, PbSnTe:In, MIS-transistor, negative photoconductivity, detector of radiation.

DOI: 10.21883/0000000000

Optical, galvanomagnetic, and dielectric properties of Pb_{1-x}Sn_xTe ($x = 0-1$) have been studied in detail since the early 1960s; its band structure; phase transitions, thermoelectric phenomena, etc, have also been examined. Thermal converters, photodiodes, and lasers with an operating range extending to extreme IR wavelengths have been constructed based on PbSnTe. The results of this research have been summarized in numerous books and review papers (see, e.g., [1–4]). It stands out as unusual against this background that the studies of metal–insulator–semiconductor (MIS) structures are so scarce and limited to measurements of capacitance ($C-V$) and conductivity ($G-V$) of PbTe-based ($x = 0$) samples only (see, e.g., [5,6]). No research data on MIS transistors (MISTs) based on PbSnTe have been published. This may be attributed to the high values of static permittivity ($\epsilon > 400$ for $x = 0$ and $\epsilon \sim 10^4$ and higher at $x > 0$) and carrier density $n_0(p_0)$ of Pb_{1-x}Sn_xTe. It has been discovered in the late 1970s that the carrier density in a certain range of x values decreases by several orders of magnitude (down to the intrinsic one [4,7]) under indium doping, thus simplifying the fabrication of PbSnTe-based MISTs. Research into the properties of PbSnTe as a crystalline topological insulator with surface Dirac states forming in the region of x with band inversion (see, e.g., [2], pp. 233–236) has been initiated circa 2010. This makes the technology of PbSnTe-based MISTs even more appealing, since MIST properties are also tied directly to the surface conditions. However, studies into PbSnTe-based MISTs have not been especially active up until now.

We have fabricated and examined the first MISTs based on three PbSnTe:In films of different conductivity formed by molecular beam epitaxy on (111)BaF₂ substrates. The procedure of MIST fabrication was detailed in [8], where a MIST based on a PbSnTe:In film with the highest conductivity and a relative variation of current in the channel under the influence of U_{gate} of about 0.07–0.08 was studied. This variation is approximately 10² times smaller than the one demonstrated in the present study, and the channel resistance for a MIST based on a PbSnTe:In film with the lowest conductivity varied under U_{gate} by a factor as high as $\sim 10^5$ [9].

Samples prepared for measurements were positioned within a metal chamber that shielded them from background radiation and was kept either in liquid helium or in its vapor. A radiation source was also mounted inside the chamber and was calibrated at $T = 4.2$ K with the use of a chip CdHgTe photodiode. The schematic circuit and the photographic image of the studied MIST are shown in the inset of Fig. 1. The main panel of Fig. 1 presents the dependences of „the Hall“ density n_0 and mobility μ_n of the initial Pb_{0.72}Sn_{0.28}Te:In film with a thickness of 1.35 μ m and an indium concentration of ~ 0.6 at.% on $1/T$. The $\mu_n(1/T)$ for a bulk single crystal [7] are shown for comparison. A high maximum mobility value $\mu_n \sim 3.8 \cdot 10^4$ cm² · V⁻¹ · s⁻¹ (curve 2), similarities in the behavior of curves 2, 3, and reflected high-energy electron diffraction data obtained in PbSnTe:In growth confirm that the initial film was of a high crystalline quality.

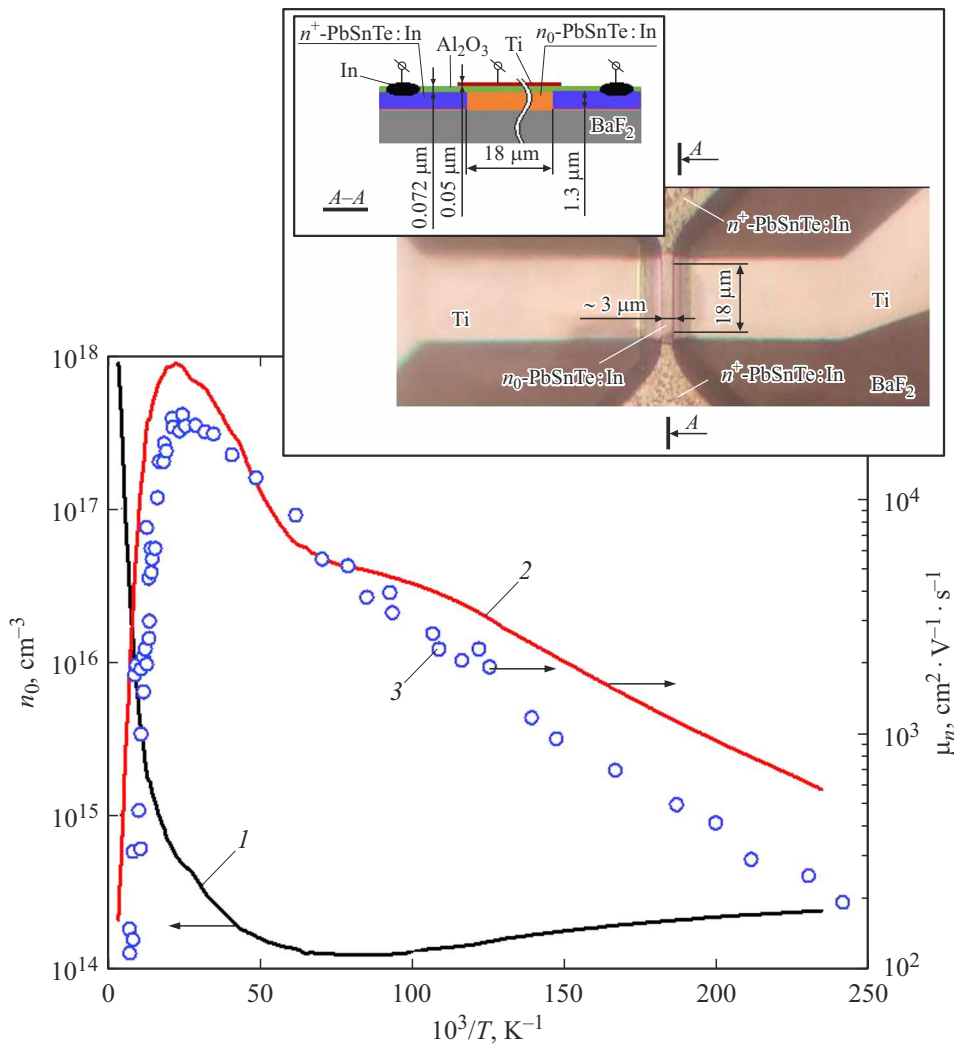


Figure 1. Dependences of „the Hall“ density $n_0 = -1/qR_H$ (1) and mobility $\mu_n = -R_H\sigma$ (2) on $1/T$ for the PbSnTe:In film used in the present study (q is the electron charge and R_H and σ are the Hall coefficient in field $B = 0.2$ T and conductivity, respectively). 3 — Dependence $\mu_n(1/T)$ from one of the first studies into the properties of low-conductivity PbSnTe:In [7]. The schematic MIST circuit and the photographic image of the near-channel region are shown in the inset.

Figure 2 shows $I_{ds}(1/T)$ curves under cooling (1, 3) and heating (2) for $U_{gate} = 0$. Dependences 1, 3 were measured at drain–source voltage $U_{ds}^{(1,3)} = 0.02$ V, while dependence 2 corresponds to $U_{ds}^{(2)} = 1.56$ V. The measured I_{ds} values (curve 2) are multiplied by ratio $U_{ds}^{(1,3)}/U_{ds}^{(2)} \cong 0.0128$. Curve 3 was calculated based on dependence $\sigma(T)$ of the initial film with the MIST channel geometry taken into account. All curves differ by no more than $\pm 10\%$ at $T > 60$ K. A considerable discrepancy between curves 1 and 3 at $T < 60$ K is apparently attributable to the difference in PbSnTe:In surface conditions: this surface is free for curve 3 and is covered by Al_2O_3 for curve 1. Curves 1 and 2 differ by a factor up to 10^6 near $T \sim 4.2$ K. This is related to the fact that measurements under illumination (see Fig. 3) were performed prior to heating. The differences between curves in Fig. 2 are evidently attributable to the presence of trap levels and their

recharging under illumination and temperature variations. It appears that at least a fraction of traps have ionization energies ΔE_t comparable to $(1-3)kT$ at $T = 60$ K (i.e., $\Delta E_t \sim 0.005-0.015$ eV).

Figure 3, a shows $I_{ds}(t)$ at $T = 4.2$ K and $U_{gate} = 0$, while the upper fragment of Fig. 3, b presents $I_{ds}(t)$ under step variation of $U_{gate}(t)$, which is shown in the lower fragment. The sections of curves measured under illumination are highlighted in red (in the online version of the paper); the moments of illumination switching are indicated by \uparrow (on) and \downarrow (off). The value of $U_{ds} = 0.02$ V is changed to $U_{ds} = 1.56$ V in Fig. 3, a at $t \sim 1630$ s. A section of the dependence with a negative photoconductivity (NPC) is shown in linear scale in the inset of this figure. The key element of Fig. 3, a is the giant NPC with I_{ds} decreasing by a factor up to $\sim 10^4$ under illumination. The features of $I_{ds}(t)$ related to illumination switching are revealed in the

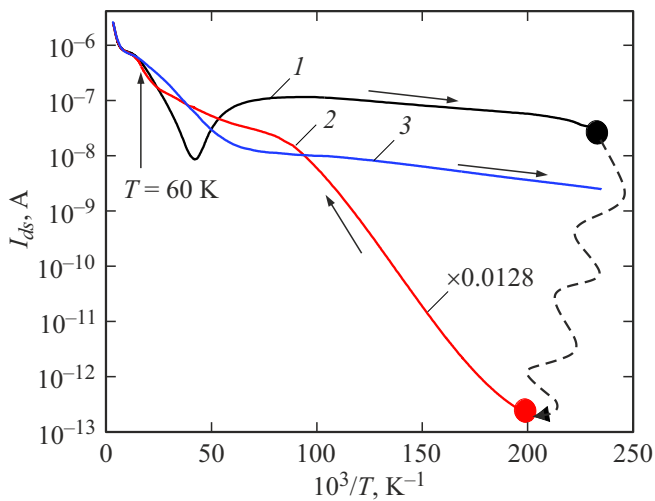


Figure 2. Dependences of MIST channel current $I_{ds}(1/T)$ without illumination under cooling (1, 3) and heating (2). The direction of temperature variation is indicated by arrows next to curves. See text for details. The dashed curve represents schematically the transition from a „conductive“ state (dot on curve 1) to a „high-resistance“ one (dot on curve 2) after illumination.

inset. At $U_{ds} = 1.56$ V (Fig. 3, a), a series of local features in the NPC section was observed under constant illumination.

A similar NPC effect was observed for PbSnTe:In films with close characteristics [10], although the relative variation of current at NPC was 10–100 times lower. A qualitative model similar to the one utilized in [11] was used to characterize NPC. This model implies the presence of relatively wide-gap inclusions with deep trap levels in

PbSnTe:In. When non-equilibrium electrons are trapped by them, the conductivity in a narrower-gap „matrix“ decreases. The results obtained in the present study clearly indicate that traps play an important (even pivotal) role in the observed effects, which may be interpreted adequately even on a qualitative level only on the assumption that different types of traps are present in the material. Specifically, the time constant of the transient process in Fig. 3, b decreases by a factor of approximately 25 as one moves from region I to region IV. It is possible if certain deep levels get filled. This may also be the reason why long-duration (with time constant $\tau > 0.5$ s) transient processes are lacking at $t > 1100$ s in Fig. 3, b. The most surprising result is that the influence of ΔU_{gate} on ΔI_{ds} becomes less pronounced while $I_{ds}(t)$ decreases in the NPC region. Roughly speaking, $\Delta U_{gate} \sim \Delta \sigma_s$ in the field effect, where $\Delta \sigma_s$ is the variation of surface charge density near the semiconductor–insulator interface. In turn, $\Delta \sigma_s = \Delta \sigma_{st} + \Delta \sigma_{sf}$, where $\Delta \sigma_{st}$ and $\Delta \sigma_{sf}$ are the variations of localized and free surface charge density, respectively, and $\Delta I_{ds} \sim \Delta \sigma_{sf}$. There are two limit approaches to explaining qualitatively the ΔI_{ds} reduction at constant ΔU_{gate} . The first one implies a strong (two orders of magnitude or more) $\Delta \sigma_{sf}$ reduction at a constant $\Delta \sigma_s$ within NPC sections. This means that the density of traps, which govern the value of $\Delta \sigma_{st}$, increases greatly (and/or the properties (population) of these traps change) at NPC. The second approach is that $\Delta \sigma_s$ itself decreases by a factor of 100 or more, which is possible if ϵ grows in PbSnTe:In under illumination. This should be manifested as a photocapacitance effect (PCE), which was observed in [12] for films and in [13] for a bulk PbSnTe:In single crystal (with the capacitance of samples varying by a factor of 100 or more). The authors of [13] believe that this

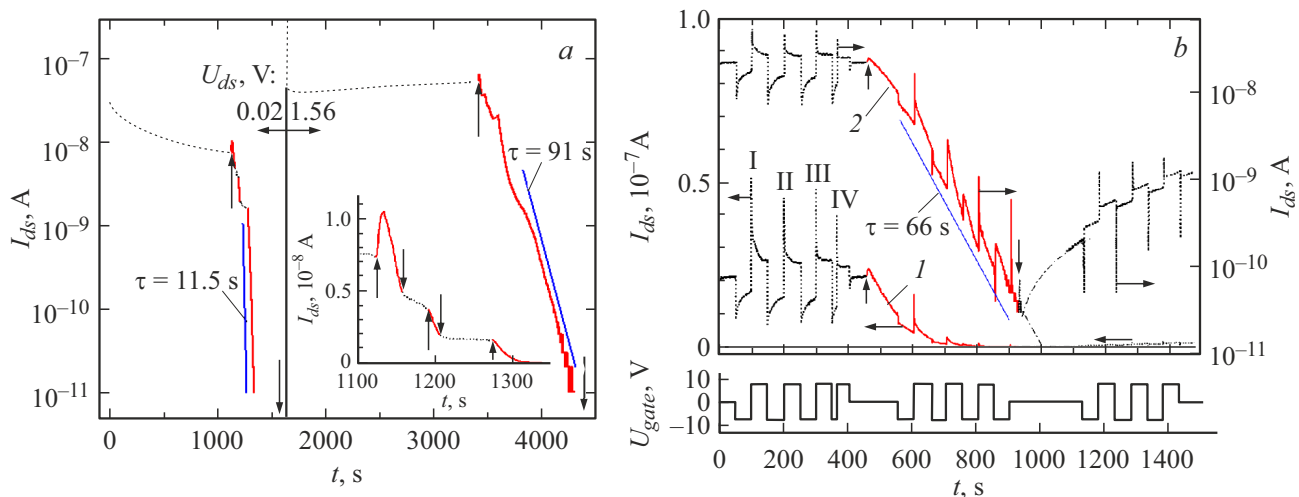


Figure 3. Temporal dependences $I_{ds}(t)$ at $T = 4.2$ K. a — Voltage $U_{gate} = 0$, b (upper fragment) — step variation of $U_{gate}(t)$ (shown in the lower fragment). The sections of curves measured under illumination are highlighted in red (in the online version of the paper). The segments near curves $I_{ds}(t)$ correspond to dependences $I \sim \exp(-t/\tau)$ (with τ values indicated next to them). Curves 1 and 2 in the right panel are presented in linear and semi-logarithmic scales, respectively, and horizontal arrows next to these curves point at the corresponding scales on ordinates axes. Numbers I–IV denote the regions of $I_{ds}(t)$ relaxation after the same U_{gate} switching. See text for additional details.

giant PCE is induced by the formation of states of an unclear nature under illumination, while an increase in ϵ was assumed to be the cause in [12]. Whichever is true, the PCE itself is an undeniable fact and is likely to be the cause of the effect observed in the present study.

We note in conclusion that the detectivity of a MIST as a prototype radiation detector (RD) was also estimated in the present study by analyzing $I_{ds}(t)$ around the moments when illumination was switched on: $D_{\lambda=25\mu\text{m}}^* \sim 7 \cdot 10^{16} \text{ cm} \cdot \text{Hz}^{0.5} \cdot \text{W}^{-1}$ under background-free conditions with accumulation time $\tau \sim 0.5 \text{ s}$. This corresponds to threshold flux $P_{\lambda=25\mu\text{m}}^1 \sim 1.5 \cdot 10^{-19} \text{ W} \cdot \text{Hz}^{-0.5}$ for an RD $\sim 100 \times 100 \mu\text{m}$ in size. The indicated value is comparable to the characteristics of state-of-the-art extreme IR and submillimeter RDs under low background fluxes (see [3], pp. 936, 981, 999). It is conceivable that further advances in the technology of PbSnTe:In-based MISTs will help solve the important problem of „delayed photoconductivity“ in RDs based on PbSnTe:In [14].

Funding

This study was supported by grants No. 20-02-00324 (electrophysical measurements) and No. 19-29-12061 (sample fabrication) from the Russian Foundation for Basic Research.

Conflict of interest

The authors declare that they have no conflict of interest.

References

- [1] Yu.I. Ravich, B.A. Efimova, I.A. Smirnov, *Metody issledovaniya poluprovodnikov v primenenii k khal'kogenidam svintsya PbTe, PbSe i PbS* (Nauka, M., 1968) (in Russian).
- [2] G. Springholz, *Molecular beam epitaxy: From research to mass production*, 2nd ed. (Elsevier, Netherlands, 2018), p. 211–276, 233–236.
- [3] A. Rogalski, *Infrared and terahertz detectors*, 3rd ed. (CRC Press, Boca Raton, 2019), p. 527–578, 936, 981, 999.
- [4] B.A. Volkov, L.I. Ryabova, D.R. Khokhlov, *Phys. Usp.*, **45** (8), 819 (2002). DOI: 10.1070/PU2002v045n08ABEH001146.
- [5] D.A. Lilly, D.E. Joslin, H.K.A. Kan, *Inf. Phys.*, **18** (1), 51 (1978). DOI: 10.1016/0020-0891(78)90010-6
- [6] P.H. Zimmermann, M.E. Mathews, D.E. Joslin, *J. Appl. Phys.*, **50**, 5815 (1979). DOI: 10.1063/1.326725
- [7] B.M. Vul, I.D. Voronova, G.A. Kalyuzhnaya, T.S. Mamedov, T.Sh. Ragimova, *JETP Lett.*, **29** (1), 18 (1979).
- [8] A.E. Klimov, V.A. Golyashov, D.V. Gorshkov, E.V. Matyushenko, I.G. Neizvestny, G.Yu. Sidorov, N.S. Paschin, S.P. Suprun, O.E. Tereshchenko, *Semiconductors*, **56** (2), 182 (2022). DOI: 10.21883/SC.2022.02.53273.30.
- [9] A.E. Klimov, A.Yu. Mironov, I.O. Akhundov, V.A. Golyashov, D.V. Gorshkov, D.V. Ishchenko, N.S. Pashchin, G.Yu. Sidorov, S.P. Suprun, A.S. Tarasov, E.V. Fedosenko, O.E. Tereshchenko, in *Sbornik tezisov dokladov XV Rossiiskoi konferentsii po fizike poluprovodnikov* (Nizhnii Novgorod, 2022), p. 67 (in Russian). <https://semicond2022.ru/file/29/b86bdcf0/abstracts.pdf>
- [10] A.N. Akimov, A.E. Klimov, S.V. Morozov, S.P. Suprun, V.S. Epov, A.V. Ikonnikov, M.A. Fadeev, V.V. Rummyantsev, *Semiconductors*, **50** (12), 1684 (2016). DOI: 10.1134/S1063782616120022.
- [11] R.A. Hopfel, *Appl. Phys. Lett.*, **52** (10), 801 (1988). DOI: 10.1063/1.99288
- [12] A.E. Klimov, V.N. Shumskii, *Prikl. Fiz.*, No. 3, 74 (2004) (in Russian).
- [13] A.E. Kozhanov, A.V. Nikorich, L.I. Ryabova, D.R. Khokhlov, *Semiconductors*, **40** (9), 1021 (2006). DOI: 10.1134/S1063782606090053.
- [14] A.G. Klimenko, A.E. Klimov, I.G. Neizvestny, A.A. Fratsuzov, V.N. Shumsky, in *Narrow gap semiconductors*, ed. by S.C. Shen, D.V. Tang, G.V. Zheng, G. Bauer (World Scientific, 1997), p. 164.